

Supplementary material for

Modeling anaerobic soil organic carbon decomposition in Arctic polygon tundra: insights into soil geochemical influences on carbon mineralization

Jianqiu Zheng¹, Peter E. Thornton^{2,3}, Scott L. Painter^{2,3}, Baohua Gu², Stan D. Wullschleger^{2,3}, David E. Graham^{1,3}

¹Biosciences Division, Oak Ridge National Laboratory, Oak Ridge TN, 37931 USA

²Environmental Sciences Division, Oak Ridge National Laboratory, Oak Ridge TN, 37931 USA

³Climate Change Science Institute, Oak Ridge National Laboratory, Oak Ridge TN, 37931 USA

Correspondence to: David E. Graham (grahamde@ornl.gov)

Table S1 Summary of soil microcosm studies and physicochemical characteristics

Core Sample ID	Type	Soil Layer	Depth	Incubation	Water content (g g ⁻¹ dwt.)	pH	SOC (C wt %)	Treatment ID
NGADG0017	LCP-Center	Organic	0-21.5 cm	Anoxic	9.62	5.0	38.5	LCP-C1-O
		Mineral	22-54 cm	Anoxic	0.64	4.8	14.7	LCP-C1-M
NGADG0073	LCP-Center	Mineral	15-40 cm	Anoxic	1.06	5.9	17.58	LCP-C2-M
		Permafrost	55-82 cm	Anoxic	0.43	7.1	1.97	LCP-C2-P
NGADG0005	LCP-Ridge	Organic	0-8 cm	Anoxic	3.67	5.2	38.9	LCP-R-O
		Mineral	8-42 cm	Anoxic	0.74	4.5	14.7	LCP-R-M
NGADG0009	LCP-Trough	Organic	0-19 cm	Anoxic	2.48	5.2	20.6	LCP-T-O
		Mineral	25-69 cm	Anoxic	0.79	5.0	8.1	LCP-T-M
NGADG0003	FCP-Center	Organic	8-28 cm	Oxic	0.44	4.2	18.6	FCP-C-O
		Transitional	38-48 cm	Anoxic	2.48	4.9	5.8	FCP-C-T
		Permafrost	48-68 cm	Anoxic	3.95	5.0	30.8	FCP-C-P
NGADG0043	HCP-Center	Organic	10-20 cm	Oxic	0.44	3.8	20.5	HCP-C1-O
		Mineral	20-50 cm	Anoxic	0.93	4.5	17.1	HCP-C1-M
NGADG0001	HCP-Center	Organic	10-30 cm	Oxic	0.67	4.7	20.5	HCP-C2-O
		Permafrost	50-70 cm	Anoxic	4.43	5.7	17.1	HCP-C2-P
NGADG0048	HCP-Trough	Organic	10-30 cm	Anoxic	2.20	5.1	31.0	HCP-T-O
		Mineral	30-50 cm	Anoxic	1.38	5.3	17.3	HCP-T-M

Table S2 Initial conditions used for model simulation

Treatment ID	SOC (mol)	TOTW (mL)	TOAC (mM)	pH	Fe(II) (mM)	f_{doc}	Me_biomass (mol C)	Fe_biomass (mol C)
LCP-C1-O	0.05	13.6	6.37	5.0	0.79	0.02	8e-5	2e-5
LCP-C1-M	0.11	5.9	2.78	4.8	22.23	0.01	4e-6	1e-5
LCP-C2-M	0.15	5.2	0.47	5.9	2.7	0.01	4e-6	5e-7
LCP-C2-P	0.02	2.8	4.05	7.1	5.0	0.02	5e-8	2e-7
LCP-R-O	0.10	11.8	0.06	5.2	1.62	0.02	5e-6	1e-5
LCP-R-M	0.11	6.4	2.67	4.5	22.97	0.01	2e-5	2e-5
LCP-T-O	0.07	10.7	1.03	5.2	15.67	0.02	1e-5	5e-6
LCP-T-M	0.06	6.6	1.84	5.0	7.18	0.01	8e-6	1e-5
FCP-C-T	0.02	7.1	2.15	4.9	20.24	0.02	1e-6	1e-5
FCP-C-P	0.08	8.0	10.76	5.0	17.45	0.02	2e-7	2e-6
HCP-C1-M	0.14	4.8	12.58	5.92	113.98	0.01	-	1e-9
HCP-C2-P	0.14	8.2	8.57	7.06	17.92	0.02	-	1e-9
HCP-T-O	0.26	4.9	39.87	5.1	25.62	0.01	5e-7	1e-6
HCP-T-M	0.14	5.8	2.84	5.3	20.92	0.01	2e-6	1e-8

Table S3 Estimated fermentation rate at 25°C

Treatment ID	f_{fer} (day $^{-1}$)
LCP-C1-O	1.73E-01
LCP-R-O	1.73E-02
LCP-T-O	1.73E-02
HCP-T-O	1.73E-02
LCP-C1-M	1.73E-03
LCP-R-M	1.73E-03
LCP-T-M	3.46E-03
FCP-C-T	3.46E-03
LCP-C2-M	4.32E-05
HCP-CM	4.32E-06
HCP-T-M	8.64E-07
FCP-C-P	8.64E-05
LCP-C2-P	8.64E-05
HCP-C2-P	1.73E-07

Table S4 Descriptive statistics and correlation matrix for soil attributes, labile carbon pool and estimated 60 days maximal production of CO₂ and CH₄ (gas production calculated as per gram dry soil) at +8 and -2 °C.

	1	2	3	4	5	6	7	8a/8b
1. SOC								
2. WEOC	0.80 ^a							
3. TOAC	0.62	0.69 ^a						
4. Moisture	0.69 ^a	0.82 ^a	0.78 ^a					
5. pH	-0.30	-0.15	-0.14	-0.11				
6. C/N ratio	0.07	0.06	0.17	0.05	-0.64 ^b			
7. Fe(II)	0.06	0.09	0.15	0.04	-0.35	-0.03		
8a. Max_8_CO ₂	0.75 ^a	0.72 ^a	0.55 ^b	0.81 ^a	-0.15	-0.03	-0.28	
8b. Max_2_CO ₂	0.66 ^a	0.73 ^a	0.77 ^a	0.90 ^a	-0.12	0.11	-0.24	
9a. Max_8_CH ₄	0.54 ^b	0.63 ^b	0.67 ^a	0.85 ^a	-0.13	0.19	-0.29	0.90 ^a
9b. Max_2_CH ₄	0.47	0.61 ^b	0.75 ^a	0.84 ^a	-0.09	0.22	-0.23	0.96 ^a

Note: ^a correlation is significant at the 0.01 level (two-tailed); ^b correlation is significant at the 0.05 level (two-tailed)

Table S5 ANOVA for effect of temperature and soil depth on initial production rate of CO₂ and CH₄

		<i>F</i>	<i>p</i>
CO ₂	Temperature	3.83	0.02
	Soil depth	25.93	<0.001
	Interaction	3.90	0.005
CH ₄	Temperature	3.26	0.04
	Soil depth	7.70	<0.001
	Interaction	2.29	0.07

Table S6 Temperature effects on initial production rates of CO₂ and CH₄ (*t*-test with unequal variances)

		<i>t</i>	<i>p</i>
CO ₂	Organic vs. Mineral	2.36	0.85
	Organic vs. Permafrost	3.18	<0.01
	Mineral vs. Permafrost	2.31	<0.01
CH ₄	Organic vs. Mineral	4.30	0.13
	Organic vs. Permafrost	4.30	0.09
	Mineral vs. Permafrost	2.78	0.12

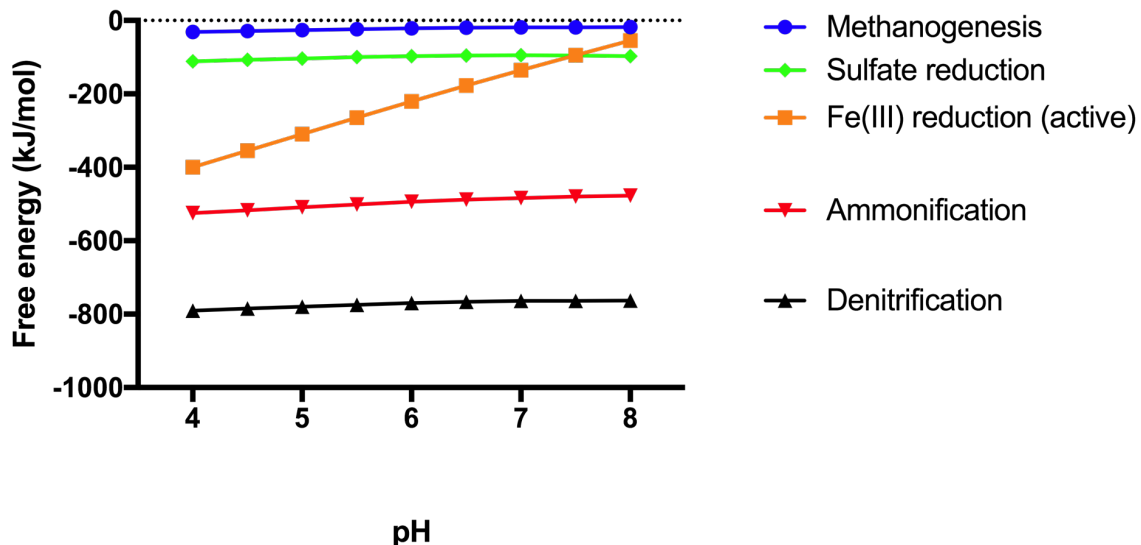


Figure S1 The Gibbs free energy of anaerobic microbial processes increases with pH. Calculated from standard free energies of reaction for acetate oxidation coupled to the indicated reduction processes (Hanselmann, 1991). Substrate and product concentrations were estimated from BEO polygon soil samples assuming 298 K temperature, 200 μM total dissolved CO_2 species, 1 mM Fe(OH)_3 equiv., 14 mM $\text{Fe}(\text{II})$, 374 μM acetate, 5.7 μM dissolved CH_4 , 160 nM NO_3^- , 28 μM NH_4^+ , and 75 μM SO_4^{2-} .

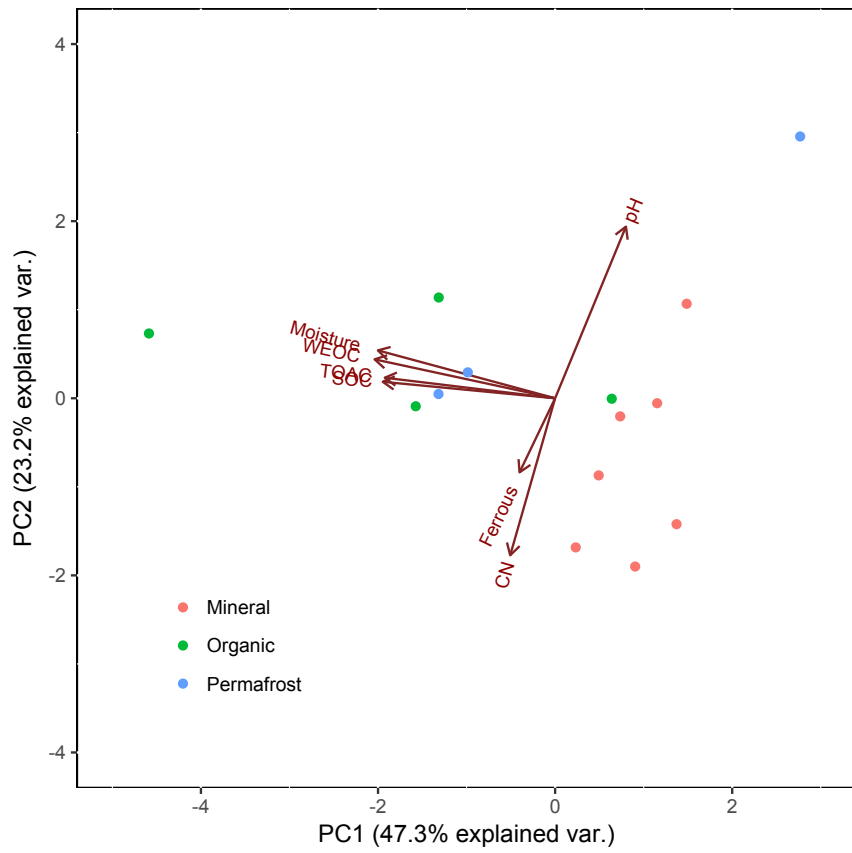


Figure S2 Multivariate analysis on soil geochemical characteristics among distinct soil depths

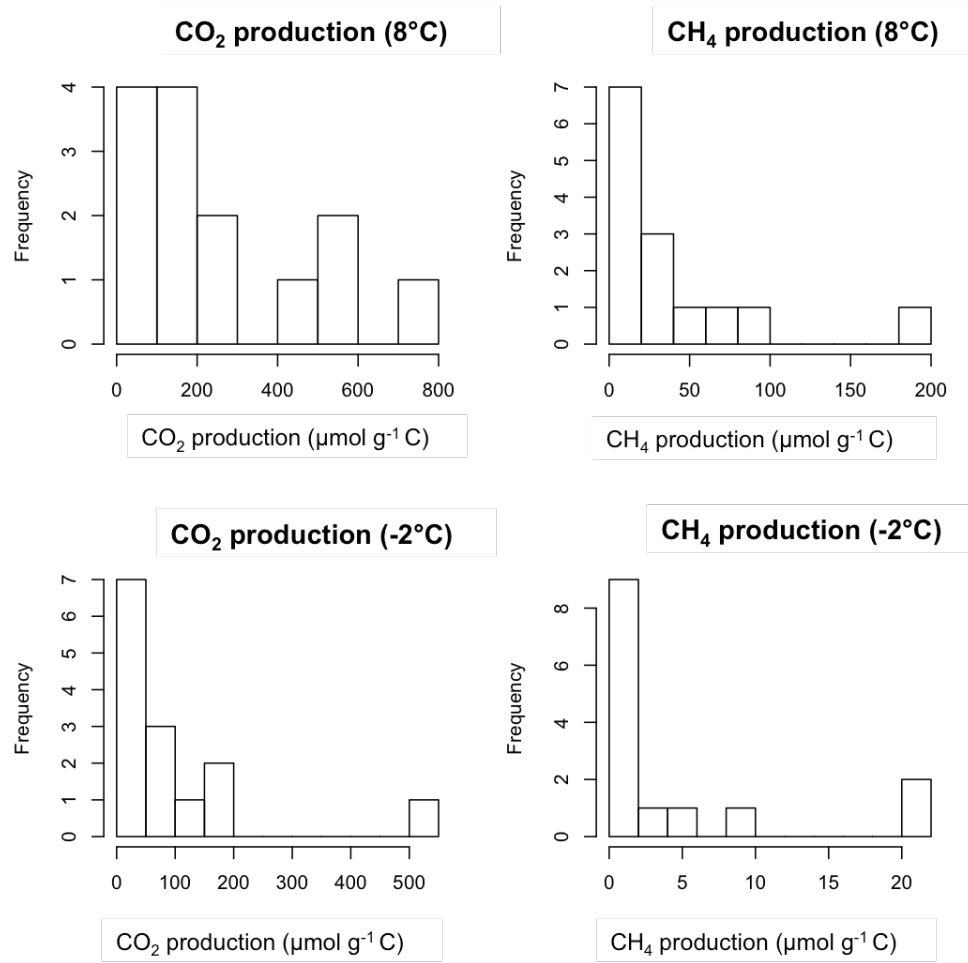


Figure S3 Data distribution of maximum CO₂ and CH₄ production among different treatments.

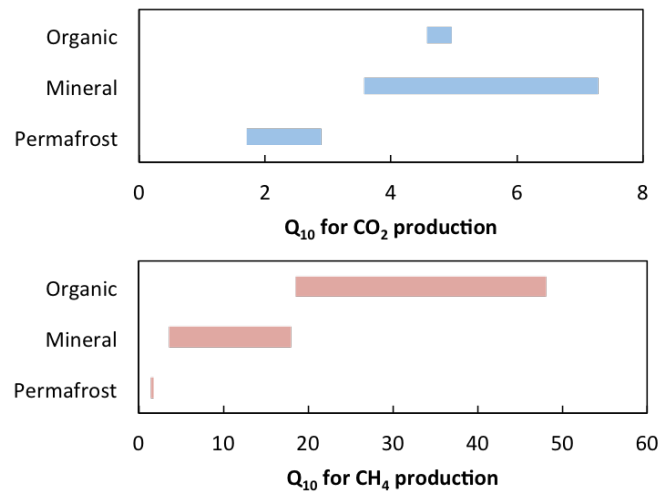


Figure S4 Temperature sensitivity of CO₂ and CH₄ production. CO₂ production rate at 4 and 8 °C were both normalized to CO₂ production rate at -2°C for each soil microtopographic feature and soil layer combination.

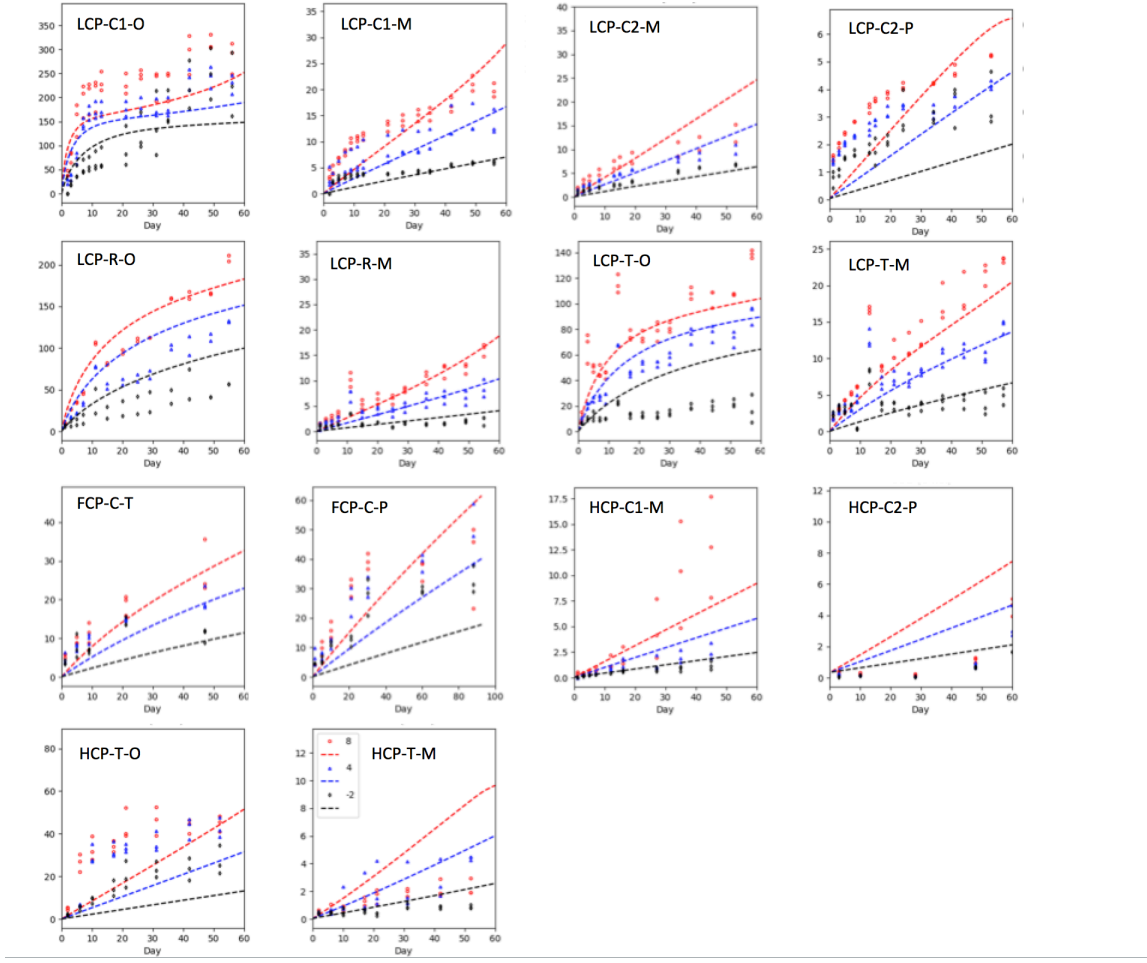


Figure S5 Comparison of observed and modeled CO₂ production from organic, mineral (transitional) and permafrost layers of different microtopographic features of LCP, FCP and HCP.

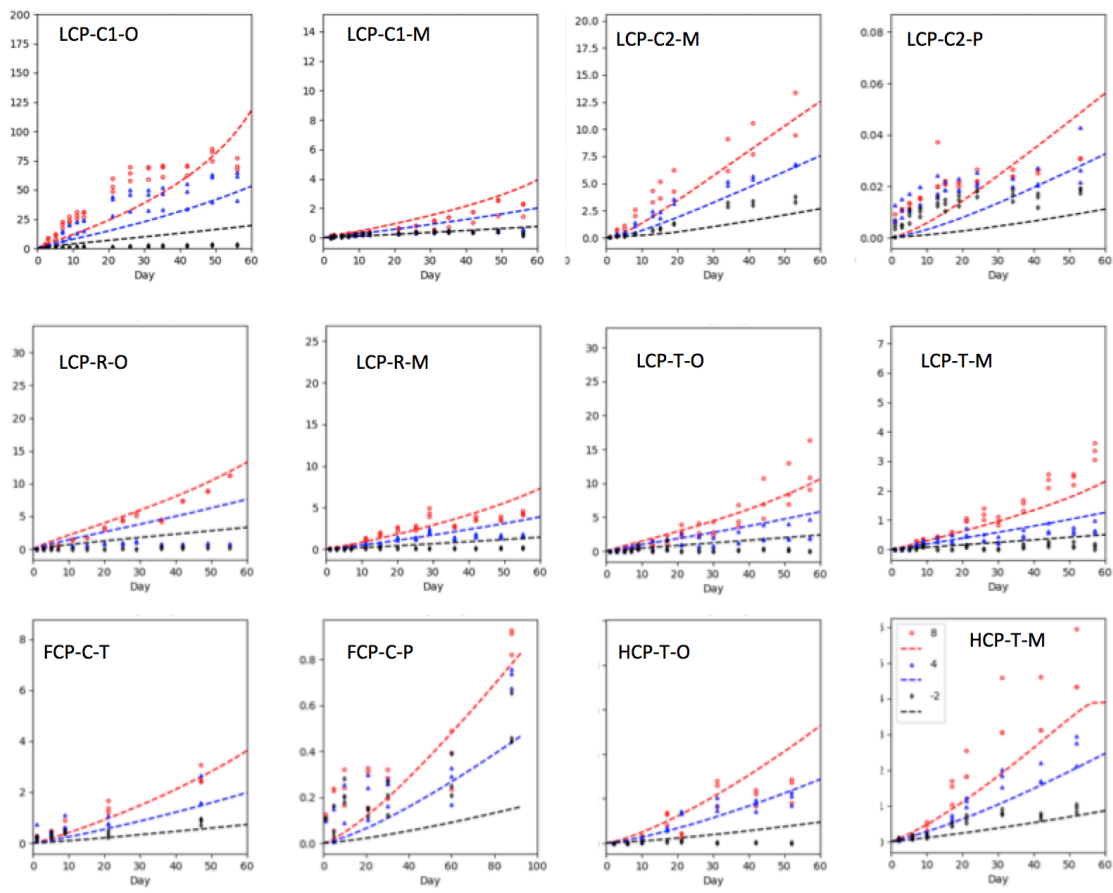


Figure S6 Comparison of observed and modeled CH₄ production from organic, mineral (transitional) and permafrost layers of different microtopographic features of LCP, FCP and HCP.

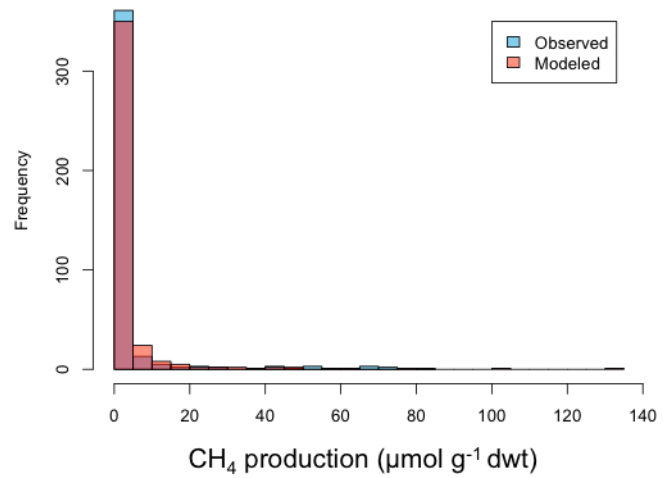
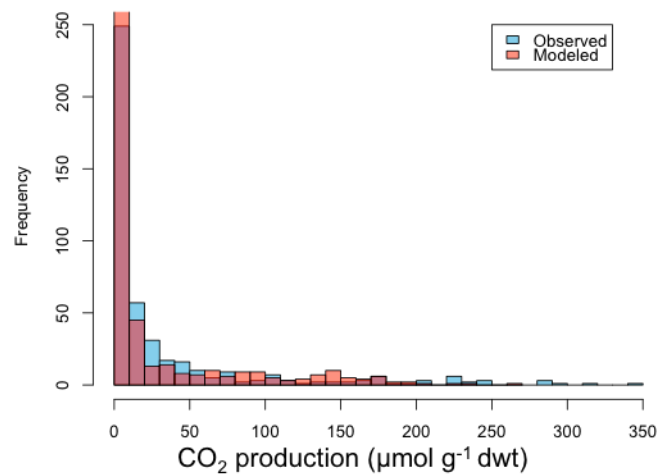


Figure S7 Comparison of data distribution between modeled and observed values for both CO_2 (upper) and CH_4 (lower) production.

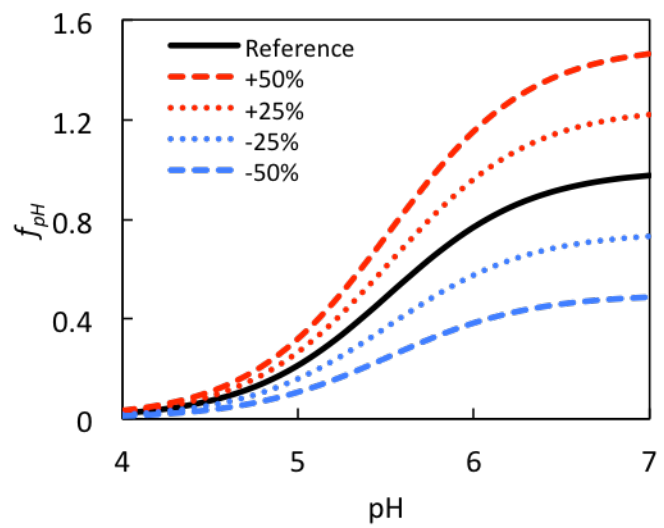


Figure S8. pH response functions used in sensitivity analysis. Perturbations of $\pm 25\%$ and $\pm 50\%$ perturbations to the final value of f_{pH} .

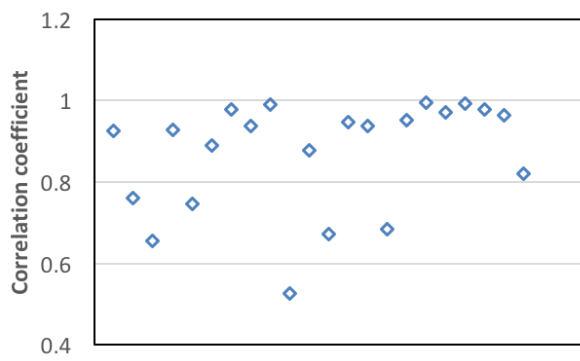


Figure S9 Correlations between Fe(II) concentration increase and pH increase during anaerobic incubations of LCP and FCP samples.